http://www.ejournalofscience.org

P-Delta Dynamic Analysis of Structures Equipped with Viscous Fluid Dampers Considering Soil-Structure Interaction

[1]Pham Nhan Hoa, [2]Chu Quoc Thang, [3]Angeli Cabaltica Doliente

[1]Department of Civil Engineering, International University - Vietnam National University - HCM

and Faculty of Civil Engineering and Applied Mechanics, HCMC University of Technology and Education,

1 Vo Van Ngan Street, Thu Duc District, Ho Chi Minh City, Vietnam.

[2]Department of Civil Engineering, International University - Vietnam National University – HCM.

[3]Department of Civil Engineering, International University - Vietnam National University – HCM.

E-mail: [1]pnhoa@hcmiu.edu.vn or 1421003@student.hcmute.edu.vn , [2]cqthang@hcmiu.edu.vn, [3]angeli.dc@hcmiu.edu.vn

ABSTRACT

The paper presents the mathematical model to find the response of a structure equipped with viscous fluid dampers (VFD) considering its P-Delta effect and soil-structure interaction (SSI). This model considers dynamic-response reduction in internal forces of beam-columns when the structure is subjected to earthquake excitation. Numerical examples show results of dynamic response of two steel buildings, VFD structures with SSI and without SSI. Some conclusions about the differences between the two structures are drawn to aid civil-engineering structural designers in resisting seismic loading.

Keywords: *Dynamics of Structures, Structural Control, P-Delta analysis, Viscous Fluid Dampers, Soil-structure Interaction.*

1. INTRODUCTION

The use of dampers to enhance seismic resistances is recently popular over the world thanks to efficiency of seismic resistances. Viscous fluid dampers are one of most useful passive devices, its reasonable and economy [4][5][22].

The superstructure of a building is deeply examined such as the shear frame model (SFM) which considers beams accompanied with slabs as rigid bodies, and the finite element method (FEM) which considers beam and column flexural stiffness and their axial stiffness. However, SFM is not proper for structures with large spans. FEM does not consider local soil conditions, and regional geology beneath its structure, the effect of pile group or distance between two piles, or the effect of axial load in a beam-column element on its flexural stiffness [6][7][8][9][10][11]. Hence, both p-delta and SSI analyses for a VFD structure provides more exact dynamic response than FEM analysis.

Dynamic properties of a structure be governed by on its natural periods which are affected by soil-structure interaction (SSI), and by its beam-column flexural stiffness (p-δ effect). The research of SSI covers several approaches such as Winkler model [13], Direct Method [12][14], or the simplest method-Lump parameter model [15][16][18].

To more reasonably evaluate efficiency of dynamic response reduction of VFD structures, a computaional model of VFD building considering P-Delta effects for beam-column elements and SSI could be analyzed.

2. THE MODEL OF VFD STRUCTURES CON P-DELTA AND SSI ANALYSIS

2.1 Computational Model

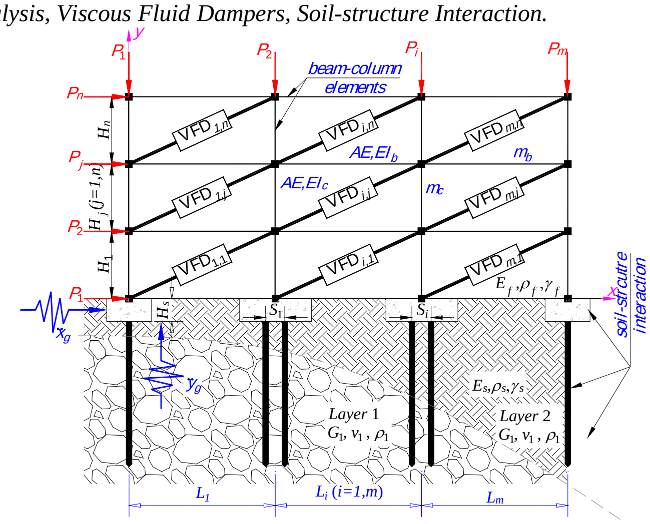

Figure 1: A VFD structure with SSI

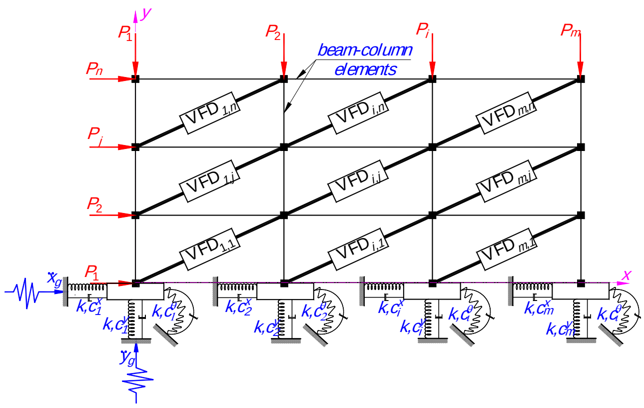

Figure 2: Mathematical model of a structure retrofitted with VFD subjected to external dynamic forces

Consider the *m*-bay, *n*-story planar frame and its pile foundation shown in Figure 1. The structure employs ($m\times n$) VFD equipment at each of the portals. The excitation consists of *n* lateral forces P_j and a horizontal and vertical earthquake loadings $\ddot{x}_g, \ddot{y}_g$. Flexural stiffnesses of the

VOL. 7, NO. 2, November 2017 ISSN 2225-7217
ARPN Journal of Science and Technology

http://www.ejournalofscience.org

beams and columns are $EI^{b}_{i,j}$ and $EI^{c}_{i,j}$, respectively. The beam-column stiffness matrix is obtained as [11]

$$\mathbf{K_e}=\frac{EI}{L}\begin{bmatrix} \frac{A}{I} & 0 & 0 & -\frac{A}{I} & 0 & 0 \\ & \frac{2(s_1+s_2)}{L^2} & -\frac{(s_1+s_2)}{L} & 0 & -\frac{2(s_1+s_2)}{L^2} & -\frac{(s_1+s_2)}{L} \\ & & s_1 & 0 & \frac{s_1+s_2}{L} & s_2 \\ & & & \frac{A}{I} & 0 & 0 \\ & & & & \frac{2(s_1+s_2)}{L^2} & \frac{(s_1+s_2)}{L} \\ sym & & & & & s_1 \end{bmatrix} \quad (1)$$

where $s_1=\sum_{n=0}^{6} a_n\rho^n$ and $s_2=\sum_{n=0}^{6} a_n\rho^n$ with

$$\begin{cases} a_6=-0.00056103 \\ a_5=0.0022397 \\ a_4=-0.0082555 \\ a_3=0.035493 \\ a_2=-0.17009 \\ a_1=1.316 \\ a_0=4 \end{cases} \quad \text{and} \quad \begin{cases} a_6=0.00054729 \\ a_5=-0.0021273 \\ a_4=0.0073511 \\ a_3=-0.027864 \\ a_2=0.10051 \\ a_1=-0.329 \\ a_0=2 \end{cases}$$

$\rho=\frac{PL^2}{\pi^2 EI}\in[-2,2]$.

From above assuming and using Da Lambert principle, differential equation governing the motion of a structure equipped with VFDs is expressed in matrix form as

$$\mathbf{M\ddot{u}+C\dot{u}+Ku=P-MI\ddot{u}_g-F_{VFD}} \quad (2)$$

where $\mathbf{M}$ is the consistent or lump mass matrix. $\mathbf{K}$ is a global stiffness matrix including the stiffness of soil-pile foundation $\mathbf{K_{SSI}}$ determined as [12][15] and of beam-column elements $\mathbf{K_{CnB}}$ determined as [1]; and $\mathbf{C}$ is the damping matrix computed using the Rayleigh fomula as [2]. $\mathbf{u}$ is a displacement vector; $\mathbf{\dot{u}}=\frac{d}{dt}\mathbf{u}$ and $\mathbf{\ddot{u}}=\frac{d^2}{dt^2}\mathbf{u}$ are velocity and acceleration vectors; $\mathbf{P}=[P_1,...,P_i,...,P_n]^T$ is an external force vector; $\mathbf{I}$ is a diagonal one matrix; $\mathbf{\ddot{u}_g}=\begin{Bmatrix}\ddot{x}_g\\ \ddot{y}_g\end{Bmatrix}$ is ground acceleration; $\mathbf{F_{VFD}}$ is a damping force vector generated by VFD [4]. value of $\mathbf{F_{VFD}}$ derives from the manufacture and does not exceed the maximum damper force [5].

2.2 Numerical Method for Computation of Motion Equation

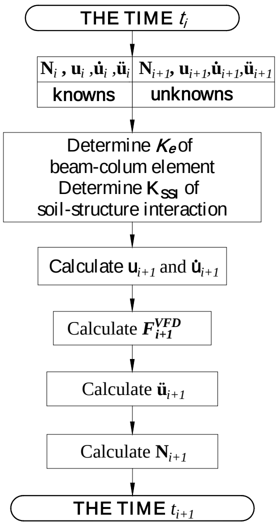

Figure 3: Algorithm of one time interval

Due mostly to non-linear forces generated from VFDs and elastic forces from beam-column elements of geometry nonlinearity, the equation (2) in time domain is resolved using the modified Newmark method. The time domain is divided to obtain discrete constant values of t_i and t_{i+1} at every Δt. The response at the time instants t_{i+1} depend on not only applied loads but also the preceding quantities of axial forces at the time t_i. The numerical method for equation (2) is illustrated in Figure 3 with the helps of MATLAB routine.

3. NUMERICAL EXAMPLES

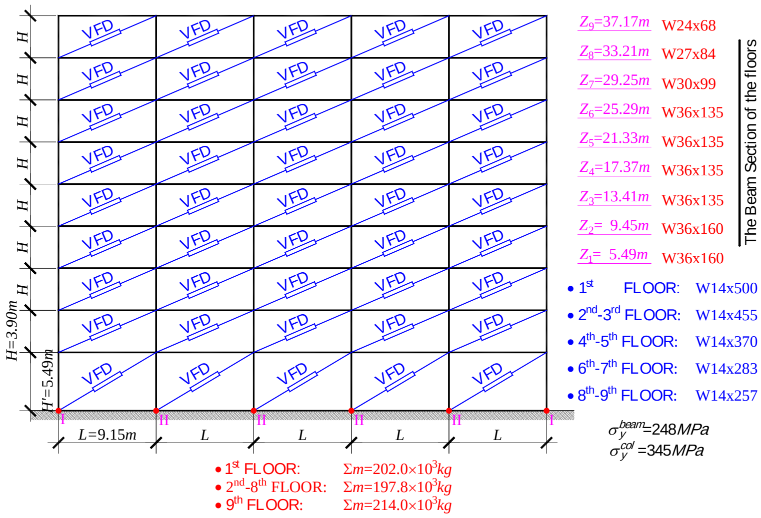

Figure 4: The Benchmark 9-story building

The 9-story steel building [23] retrofitted with VFDs has yield strength σ_y=345MPa and the damping ratios for two first modes of $\zeta_1=\zeta_2$=2%. Its dynamic properties are given in Figure 4. The first three natural periods of the structure are $T_1=1.20s$; $T_2=0.49s$; and $T_2=0.33s$. Building foundation are of two kinds I and II. Foundations I are at exterior corner columns and foundations II is at interior columns. Concrete grade for foundations is M350 (TCVN) [24] with E_p=30Gpa. The diameter of piles is $2R_p$=0.4m. The number of piles in foundation II is $n_p=3\times3=9$ with ratio of S (distance between two piles) and $2R_p$ as $\frac{S}{2R_p} = 5$.

The number of piles in foundation I is five with distance between two piles of S as well.

Layer	Soil at pile cap					
	Height H_s^{cap} (m)	Young modulus E_s^{cap} (MPa)	Poisson coef f. ν_s^{cap}	Shear modulus G_s^{cap} (MPa)	Density ρ_s^{cap} (kg/m^3)	Soil velocity c_s^{cap} (m/s)
I	2.5	30.0	0.3	11.5	1835	79
	Soil at piles					
I	35	30.0	0.40	10.7	1937	74
II		50.0	0.35	18.5	1937	98
III		70.0	0.25	28.0	1937	120
IV		90.0	0.20	37.5	1937	139

Therefore, the stiffness and damping of foundation I and II are [16][17][19][20][21][25] as

$$2k_{x,y}^{I} = k_{x,y}^{II} = 1685.1\times 10^{3}\, kN/m,$$

$$2c_{x,y}^{I} = c_{x,y}^{II} = 18756\, kN.s/m, \quad 2k_{\theta}^{I} = k_{\theta}^{II} = 28179\times 10^{3}\, kN/m,$$

$$2c_{\theta}^{I} = c_{\theta}^{II} = 81392\, kN.s/m$$

The ElCentro earthquake [3] acts on the building along the x axis with peak ground acceleration (PGA) of $(\ddot{x}_g)_{\max} = 0.35g$ (Figure 5). Analysis duration is 35 seconds with constant time intervals of Δt=0.00125s.

The response of the structure are analysized into two groups of non-controlled and VFD controlled structures as Table 1.

Table 1: Analyzed Cases

Name of cases	Analysis combined			
	Linear	P-Δ	SSI	VFD
(LIN without SSI)$_{NCT}$	✓			
(LIN with SSI)$_{NCT}$	✓		✓	
(P-Δ without SSI)$_{NCT}$		✓		
(P-Δ with SSI)$_{NCT}$		✓	✓	
(LIN without SSI)$_{VFD}$	✓			✓
(LIN with SSI)$_{VFD}$	✓		✓	✓
(P-Δ without SSI)$_{VFD}$		✓		✓
(P-Δ with SSI)$_{VFD}$		✓	✓	✓

the VFD in one portal as $\begin{cases} C_j^{VFD} = 2\times 10^{6}\, Ns/m; \alpha_j = 1 \\ f_{j,\max}^{VFD} = 60kN \end{cases}$

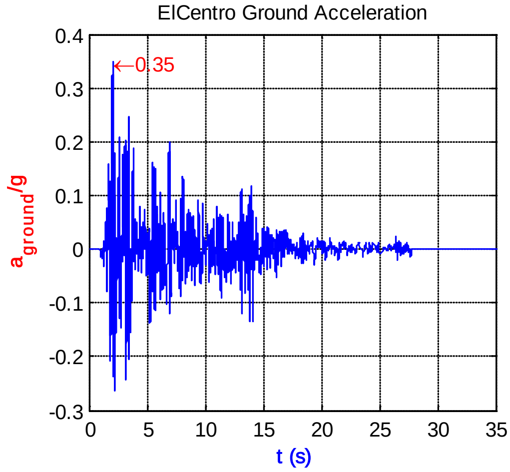

Figure 5: Time history of the ElCentro ground acceleration [3]

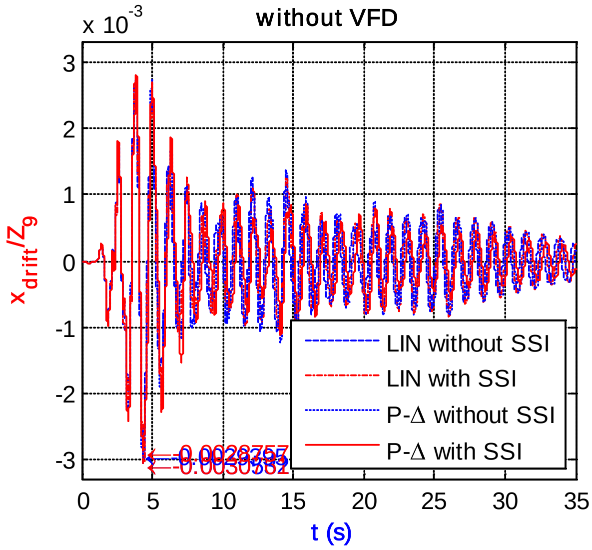

Figure 6: Story drift response versus time without VFD

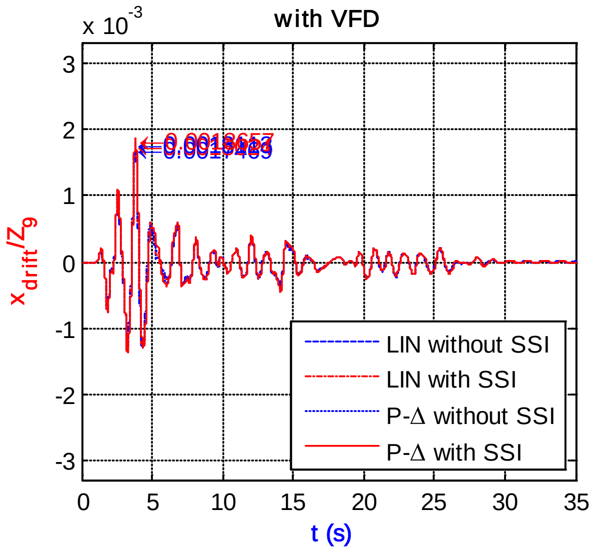

Figure 7: Story drift response versus time with VFD

VOL. 7, NO. 2, November 2017 ISSN 2225-7217
ARPN Journal of Science and Technology

http://www.ejournalofscience.org

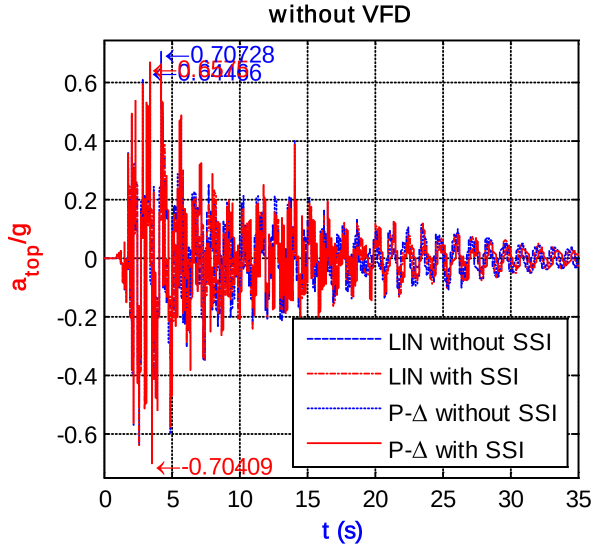

Figure 8: Top acceleration response versus time without VFD

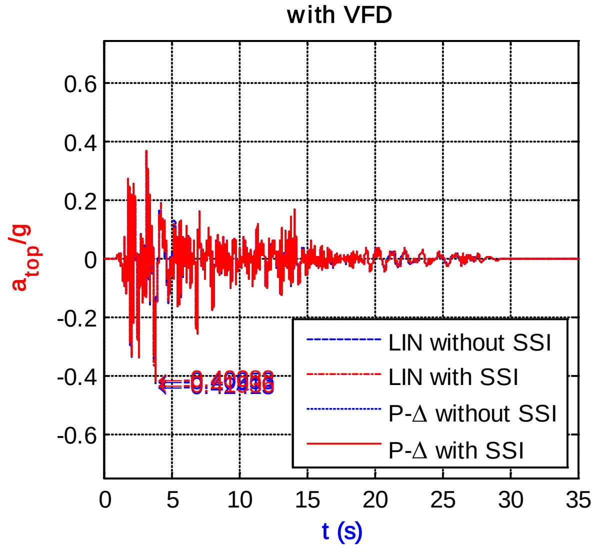

Figure 9: Top acceleration response versus time with VFD

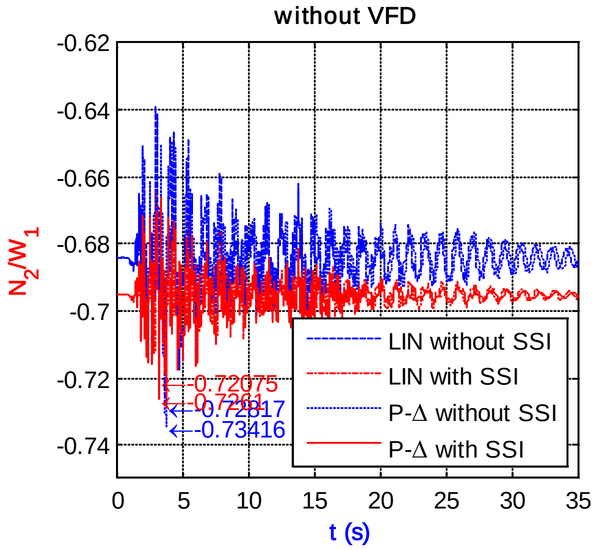

Figure 10: Axial force of the second column without VFD

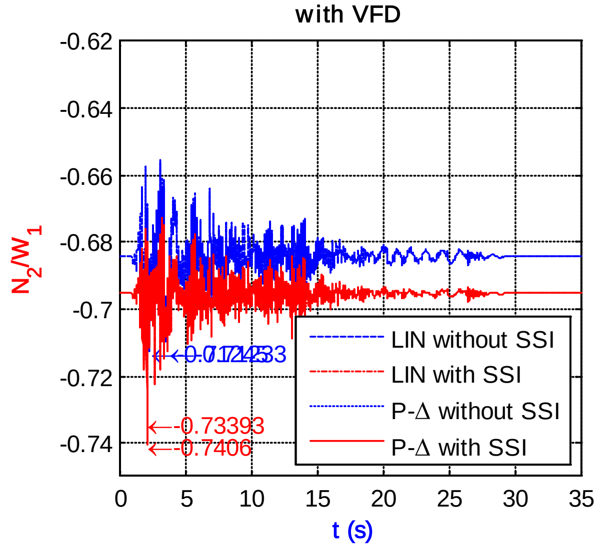

Figure 11: Axial force of the second column with VFD

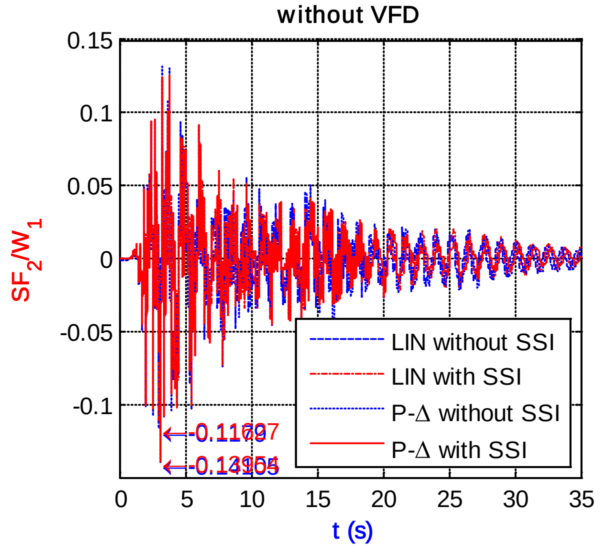

Figure 12: Shear force at the end a of the second column without VFD

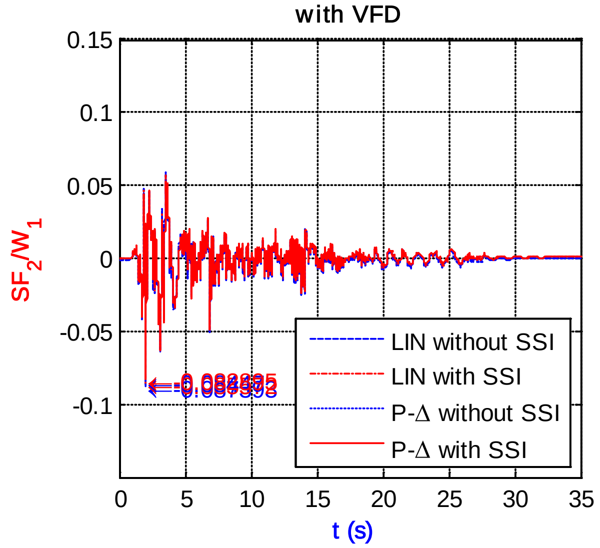

Figure 13: Shear force at the end a of the second column with VFD

VOL. 7, NO. 2, November 2017 ISSN 2225-7217
ARPN Journal of Science and Technology

http://www.ejournalofscience.org

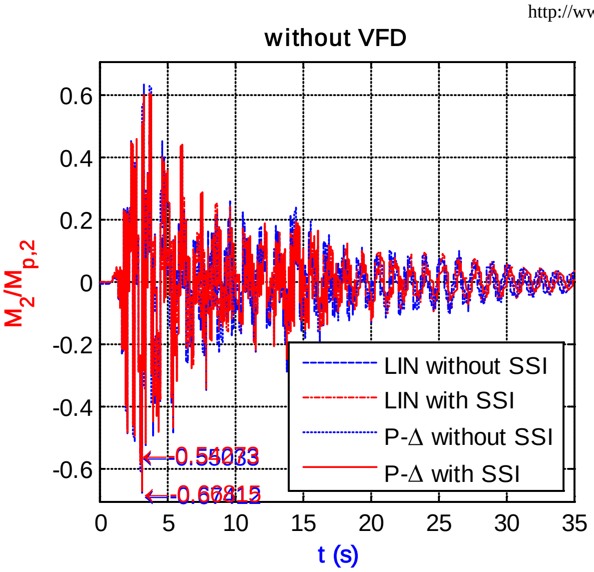

Figure 14: Moment at the end a of the second column ($M_{p,2}$=$W_{p,2}$. σ_y^{col}) without VFD

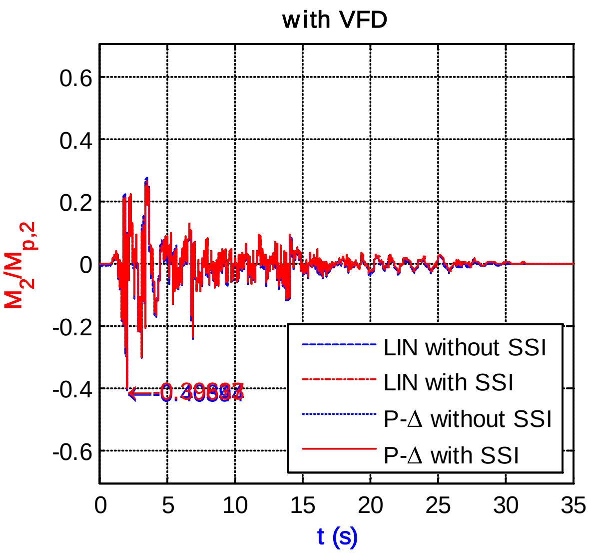

Figure 15: Moment at the end a of the second column ($M_{p,2}$=$W_{p,2}$. σ_y^{col}) with VFD

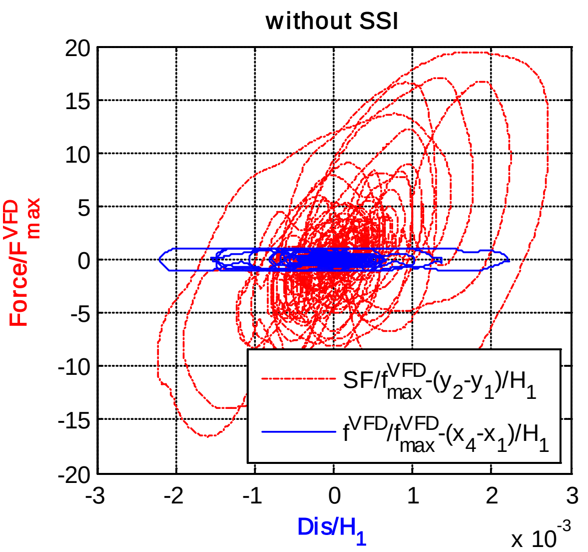

Figure 16: Hysteretic loop of Shear force and VFD without SSI

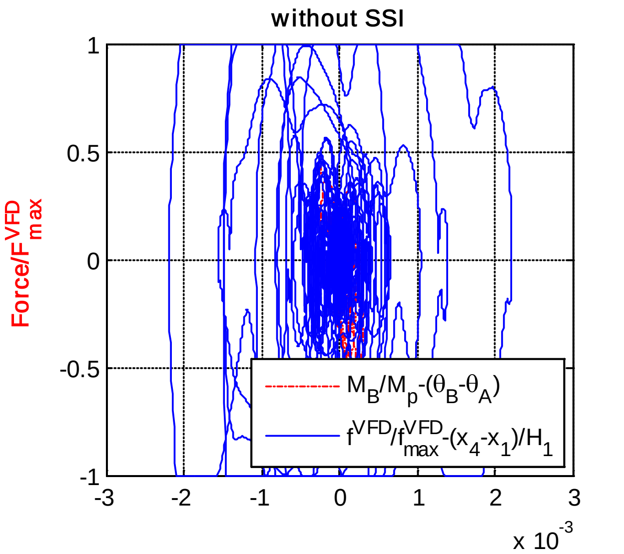

Figure 17: Hysteretic loop of Moment and VFD without SSI

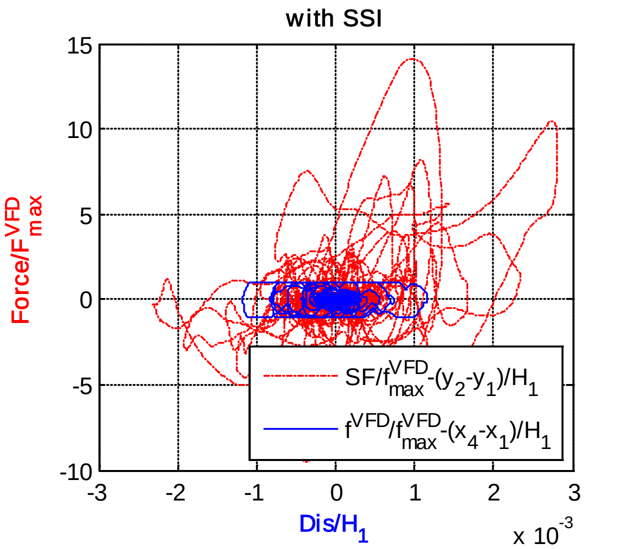

Figure 18: Hysteretic loop of Shear force and VFD with SSI

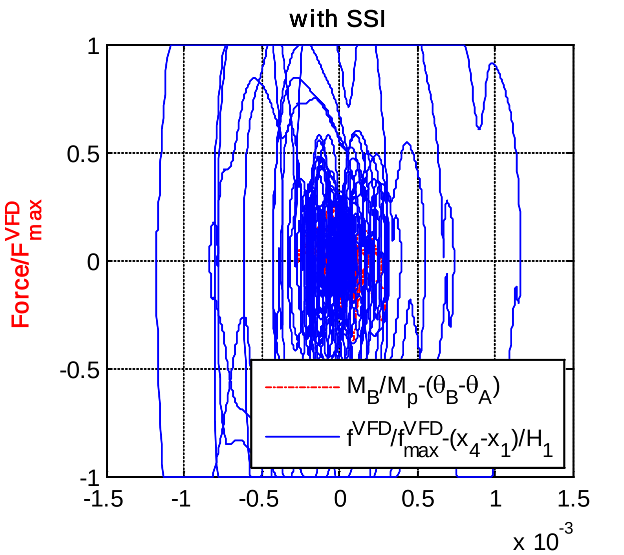

Figure 19: Hysteretic loop of Moment and VFD with SSI

VOL. 7, NO. 2, November 2017 ISSN 2225-7217
ARPN Journal of Science and Technology

http://www.ejournalofscience.org

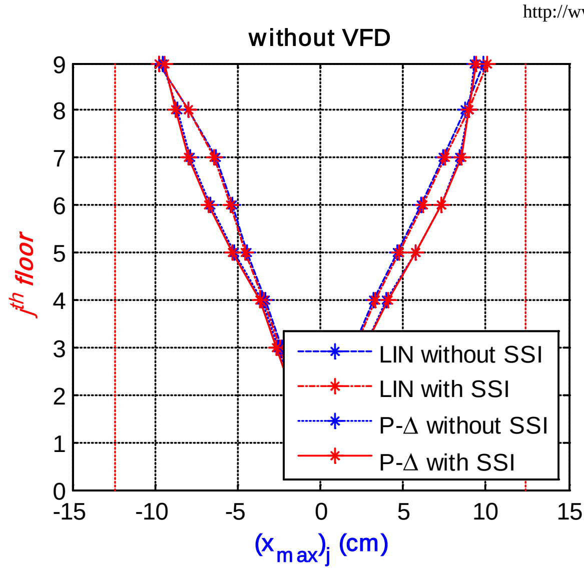

Figure 20: Maximum story drift without VFD

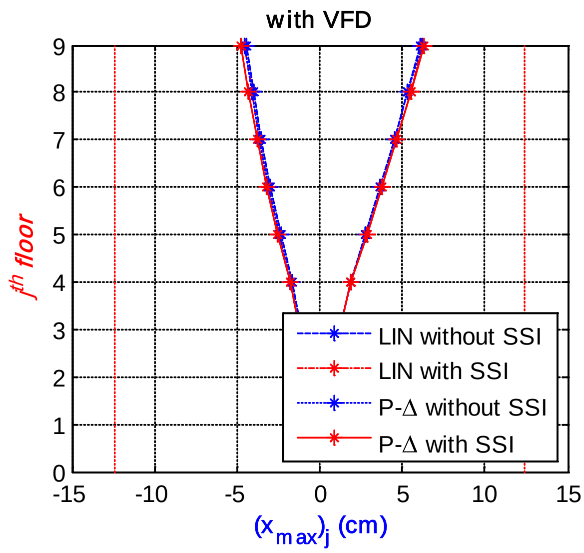

Figure 21: Maximum story drift with VFD

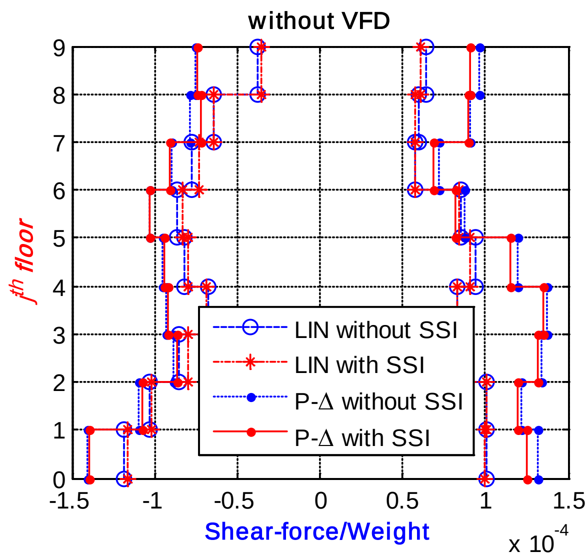

Figure 22: Ratio of columns' maximum shear forces at 1-axis to its weight without VFD

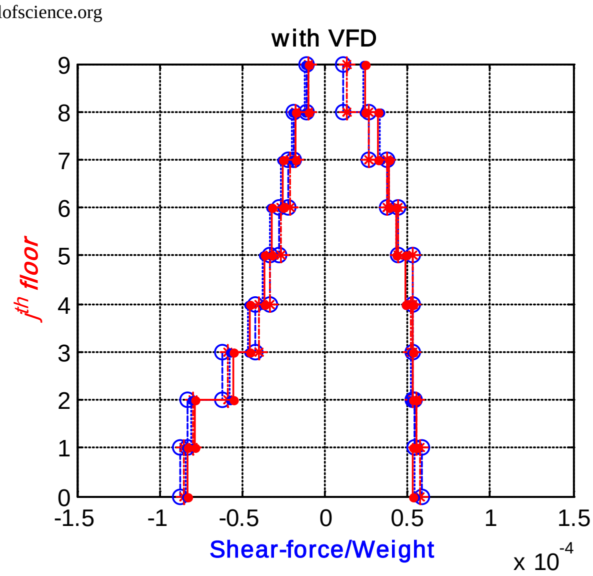

Figure 23: Ratio of columns' maximum shear forces at 1-axis to its weight with VFD

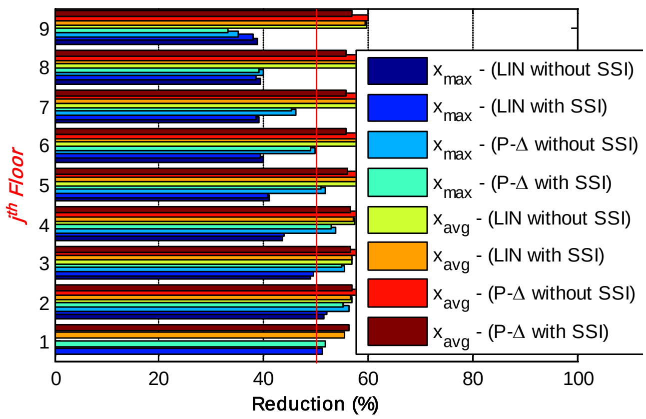

Figure 24: Dynamic reduction in horizontal displacements and accelerations of the nine floors with and without VFD

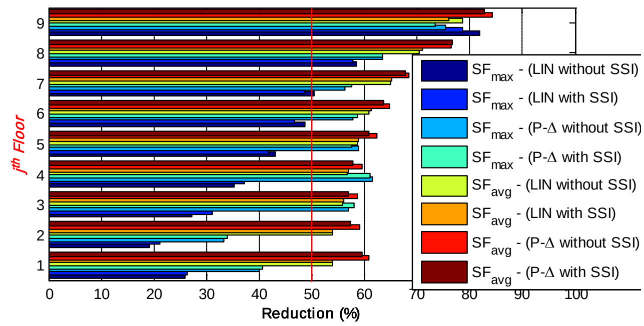

Figure 25: Dynamic reduction in Shear force at column ends at the nine floors with and without VFD

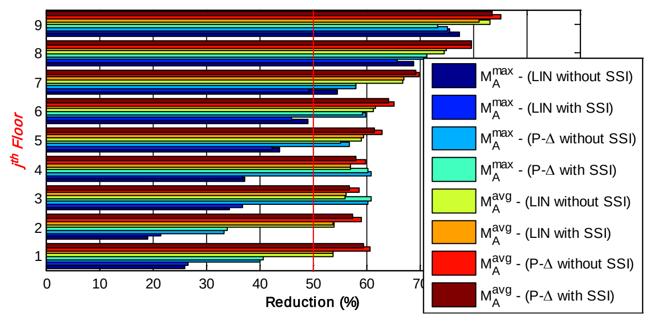

Figure 26: Dynamic reduction in Moment at column ends at the nine floors with and without VFD

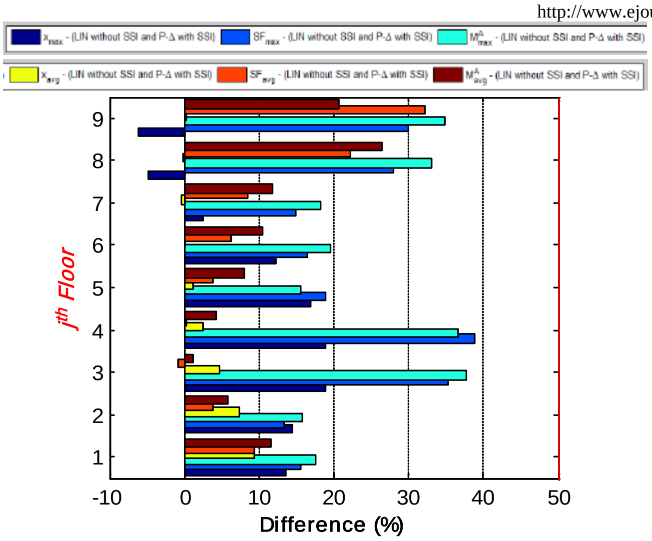

Figure 27: Difference between P-Δ analysis and linear analysis of the structure without VFD

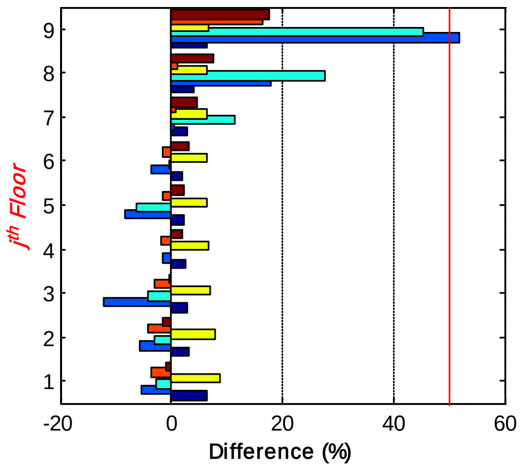

Figure 28: Difference between P-Δ analysis and linear analysis of the structure with VFD

Dynamic responses of the cases are compared in Figure 6 to Figure 28. The simplest analysis (LIN without $SSI)_{NCT}$ is not much different in maximum displacement response to other analysis consisting of (LIN with $SSI)_{NCT}$, (P-Δ without $SSI)_{NCT}$, and (P-Δ with $SSI)_{NCT}$ (Figure 6). However, it has a difference up to approximate 40% in internal forces including shear force and moment compared with (P-Δ with $SSI)_{NCT}$ (Figure 27). The acceleration responses of the four cases without VFD are the same in large PGA (peak ground acceleration) zone but dissimilar in small PGA zone (Figure 8). The axial forces of no-SSI analysis are different to the axial force of SSI analysis (Figure 10 and Figure 11). Equipped with VFD, differences between linear and P-Δ analysis, non-SSI and SSI are not considerable except 9th story (Figure 28).

The hysteretic loop of P-Δ analysis shows the nonlinearity of relationship between force and displacement (Figure 16 to Figure 19). Area of VFD hysteretic loop is many times smaller than area of shear-force hysteretic loop (Figure 18), but VFD significantly contribute to dynamic responses of VFD structures. VFD reduces 60% average, 40% max displacement (Figure 24), up to 80% shear force and moment (Figure 25 and Figure 26). To enhance response reduction or larger area of hysteretic loop, VFD could use higher maximum damper forces.

4. CONCLUSION

This paper examines linear and P-Δ analysis of VFD structures considering soil-structure interaction and subjected to seismic loading. In all cases of considering and not considering SSI, linear, and P-Δ analysis, the nine-story VFD structure expressions the acceptable dynamic reduction although it has different internal forces. In the cases of linear and P-Δ analysis, the paper illustrates more accurate evaluation of dynamic responses caused by columns' large axial forces at the 1st floor. Additionally, in the cases of linear without SSI and P-Δ with SSI, the efficiency of VFD is demonstrated in reducing dynamic responses. It in linear and P-Δ analysis is different and acceptable provided that value of VFD damper force is sufficiently large.

ACKNOWLEDGEMENT

This research is funded by International University, VNU-HCM under grant number T2016-01-CE.

REFERENCES

[1] Bathe, K.-J., Finite Element Procedures in Engineering Analysis, Prentice Hall, Englewood Cliffs, NJ., 1982.

[2] Anil K. Chopra (2012), "Dynamics of Structures", 4th edition, Prentice Hall Press.

[3] http://www.vibrationdata.com

[4] Robert J. McNamara and Douglas P. Taylor (2003), "Fluid viscous dampers for high-rise buildings", the structural design of tall and special buildings, Vol.12, pp.145–154, http://taylordevices.com/literature.html

[5] Douglas P. Taylor, Israel Katz (2004) – Seismic protection with fluid viscous dampers for the Torre Mayor, a 57-story office tower in Mexico City, Mexico, http://taylordevices.com/literature.html

[6] Chan, Siu-Lai, and Pui-Tak Chui, Non-linear static and cyclic analysis of steel frames with semi-rigid connections. Elsevier, 2000

[7] Kim, Seung-Eock, Moon-Ho Park, and Se-Hyu Choi. Direct design of three-dimensional frames using practical advanced analysis. Engineering Structures 23.11 (2001): 1491-1502.

[8] Kim, Seung-Eock, Practical second-order inelastic analysis for steel frames subjected to distributed load. Engineering Structures 26.1 (2004): 51-61.

[9] Seung-Eock Kim, Cuong Ngo-Huu, Dong-Ho Lee, Second-order inelastic dynamic analysis of 3-D steel frames. International Journal of Solids and Structures 43 (2006) 1693–1709.

ARPN Journal of Science and Technology

http://www.ejournalofscience.org

[10] Liew, J. Y. R. Advance analysis for frame design. PhD dissertation, Purdue Univ., West lafayette, Ind, 1992.

[11] Liew, J. Y. R., White, D. W., and Chen, W. F., Second-order refined plastic hinge analysis for frame design: Part II. J. Struc Engrg., ASCE, 119(11),3217-3237.

[12] Chandrakant S.Desai, Musharaf Zaman – Advanced Geotechnical Engineering, CRC Press Taylor & Francis Group, 2014.

[13] T. K. Datta, Seismic analysis of structures – Indian Institute of Technology Delhi, India, 2010.

[14] Sandro Carbonari, Francesca Dezi, Graziano Leoni – Linear soil-structure interaction of coupled wall–frame structures on pile foundations, Elsevier Ltd, 2011.

[15] Braja M. Das, G.V. Ramana – Principles of Soil Dynamics. Stamford Cengage Learning Customer & Sales Support, 2011.

[16] Milos Novak – Dynamic Stiffness and Damping of Piles. Canadian Geotechnical Journal, 1974.

[17] Wolf .J. P, Deeks – A.J.Foundation Vibration Analysis A Strength-of-Materials Approach. Elsevier, 2004.

[18] Milos Novak, M. ASCE and Bahaa El Sharnouby – Stiffness and Damping Constants of Single Piles. Journal of the Geotechnical Engineering, 7-July-1983.

[19] M. Shadlou and S. Bhattacharya – Dynamic stiffness of pile in a layered elastic continuum. S. Geotechnique, 2014.

[20] Amir M. Kaynia – Dynamics of piles and pile groups in layered soil media. Soil Dynamics and Earthquake Engineering, 1991.

[21] George Gazetas and Ricardo Dobry – Horizontal response of piles in layered soils. Journal of GeotechnicalEngineering,1984.

[22] M.C. Constantinou, M.D. Symans (1993), “Experimental study of seismic response of buildings with supplemental fluid dampers”, The structural Design of tall buildings, pp. 93-132.

[23] Y.Ohtori, R. E. Christenson, B. F. Spencer (2004), “Benchmark Control Problems for Seismically Excited Nonlinear Buildings”, Journal of Engineering Mechanics © ASCE / April 2004.

[24] TCXDVN 338:2005 about Steel Structure - Design Standard, http://www.xaydung.gov.vn/web/guest/english

[25] Dang Van Ut, Pham Nhan Hoa, Chu Quoc Thang, “Analysis of a story steel building accompanied with its pile foundation considering soil-structure interaction subjected to seismic loading”, Construction National Journal, 7-2016, pp.72-78

AUTHOR PROFILES

PHAM NHAN HOA received the master degree in computational civil engineering from Liege, Belgium in 2006. Currently, he is now a lecturer at International University – Vietnam National University, Vietnam.

CHU QUOC THANG received the PhD degree in structural engineering from TTI, Hungary in 1987. Currently, he is an Associate Professor at International University – Vietnam National University, Vietnam.

ANGELI DOLIENTE CABALTICA received her Master degree in Environmental Sanitation from Gent, Belgium in 2007 and in Water Resources Engineering and Management from Stuttgart, Germany in 2011. Currently, she is a lecturer at the International University – Vietnam National University, Vietnam.